Heat Storage Characteristics of Latent-Heat Microcapsule Slurry Using Hot Air Bubbles by Direct-Contact Heat Exchange

Hideo Inaba
Okayama University

Akihiko Horibe
Okayama University

Myoung-Jun Kim
Okayama University

Tsukamoto Hirofumi
Okayama University

Heat Storage Characteristics of Latent-Heat Microcapsule Slurry Using Hot Air Bubbles by Direct-Contact Heat Exchange*

Hideo INABA**, Akihiko HORIBE**,
Myoung-Jun KIM** and Hirofumi TSUKAMOTO**

This study deals with the heat storage characteristics of latent-heat microcapsule slurry consisting of a mixture of fine microcapsules packed with latent-heat storage material and water. The heat storage operation for the latent-heat microcapsules was carried out by the direct-contact heat exchange method using hot air bubbles. The latent-heat microcapsule consisted of *n*-paraffin as a core latent-heat storage material and melamine resin as a coating substance. The relationship between the completion time of latent-heat storage and some parameters was examined experimentally. The nondimensional correlation equations for temperature efficiency, the completion time period of the latent-heat storage process and variation in the enthalpy of air through the microcapsule slurry layer were derived in terms of the ratio of microcapsule slurry layer height to microcapsule diameter, Reynolds number for airflow, Stefan number and modified Stefan number for absolute humidity of flowing air.

Key Words: Latent-Heat Storage, Direct-Contact Heat Exchange, Paraffin, Air Bubbles, Microcapsule

1. Introduction

Recently, much attention has been paid to a new heat transfer slurry made of a mixture of water as a continuous phase and fine particles of solid-liquid phase change material as a dispersion phase, called the "functionally thermal medium" and is capable of fluidity for pipe transport and latent-heat storage[1]. Typical types of functionally thermal media are ice-water slurry and latent-heat slurry made by mixing fine encapsulated particles of paraffin and water or water solution[2]. Examples of the latter are oil/water emulsion[3], made by dispersing fine particles of paraffin wax in a water layer using surfactants, and latent-heat microcapsule water slurry[4], which consists of a mixture of fine particles of paraffin wax encapsulated by melamine resin and water. However, at low flow velocity of ice-water slurry, the ice-water slurry in a pipe results in an increase in flow drag, since the ice particles flow in contact with the upper wall surface of the pipe due to the buoyant force difference between water and ice particles. Agglomeration of ice particles in a pipe upon the functions of sintering and gathering disturbs the water-ice particle slurry flow in a transport pipe. On the other hand, the phase segregation and pipe flow blockage by agglomeration of ice particles can be avoided by using the latent-heat slurry made of a homogeneous mixture of water and fine particles of encapsulated paraffin wax. By using this type of latent-heat slurry, the temperature level and the amount of heat storage for utilization can be controlled easily by changing the type of latent-heat material and the concentration of latent-heat material with respect to the latent-heat microcapsule slurry. As a result, this type of latent-heat microcapsule slurry improves the heat storage efficiency and allows the reduction of the piping diameter and space. However, the high viscosity of the latent-heat microcapsule slurry would result in a

* Received 1st March, 2001. Japanese original: Trans. Jpn. Soc. Mech. Eng., Vol. 66, No. 645, B (2000), pp. 1487-1494 (Received 3rd March, 1999)

** Graduate School of Natural Science and Technology, Okayama University, Tsushimanaka 3-1-1, Okayama 700-8530, Japan. E-mail: inaba@mech.okayama-u.ac.jp

marked increase in the pumping power of the conventional wall-type heat exchanger.

The objective of this study is to examine the latent-heat storage characteristics of the latent-heat microcapsule slurry, which is made by dispersing fine particles packed with *n*-paraffin wax into water, for the construction of a new domestic heating and cooling system. With a view to avoiding high pumping power in the conventional wall-type heat exchanger, in the present study, we attempt to use the direct contact heat transfer method capable of a high heat transfer coefficient, in which hot air is injected into the latent-heat microcapsule slurry layer in the heat storage process. Therefore, the present experiments have been performed to examine the effects of parameters such as inlet air temperature and humidity, concentration of latent-heat material in the latent-heat slurry and the amount of latent-heat material on temperature efficiency, enthalpy difference between inlet and outlet air and the completion time of the heat storage, which are important for estimating heat and mass transfer characteristics of the latent-heat microcapsule slurry in the heat storage process. Finally, in the present study, we attempt to derive the nondimensional correlation equations of temperature efficiency, variation in air enthalpy and the completion time period in the heat storage process.

Nomenclature

a_c: thermal diffusivity of latent-heat microcapsule slurry [m^2/s]
C: concentration of latent-heat material [mass%]
Cp: specific heat [kJ/(kg·K)]
D_p: diameter of microcapsule [mm or m]
H_a: enthalpy of air [kJ/kg]
L: total latent heat [kJ/kg]
m: mass packed [kg]
N: number [-]
Q_{loss}: heat loss integrated [kJ]
Q_{mil}: latent heat integrated [kJ]
Q_{mis}: sensible heat integrated [kJ]
Q_s: condensed heat of water integrated [kJ]
Q_v: integrated sensible heat stored in vessel [kJ]
T: temperature [K]
T_c: temperature of microcapsule slurry [K]
T_{mp}: melting point [K]
T_{tp}: transition point [K]
t: time [s]
t_1: completion time period of heat storage [s]
V_o: superficial air velocity [m/s]
X_a: absolute humidity of air [kg/kg']
Z_i: height of microcapsule slurry layer [m]
Z_h: height of microcapsule slurry layer with air bubbles [m]
ε: hold-up [-]
ν: kinematic viscosity [m^2/s]
ρ: density [m^3/kg]
ϕ_a: relative humidity of air [-]

Subscripts:

a: air
c: mixture of microcapsules and water
in: inlet
m: average
mi: microcapsule latent-heat storage material
mp: melting point
tp: transition point
out: outlet
p: paraffine
s: water vapor
t: latent heat material
w: water

2. Physical Properties of Latent-Heat Microcapsule Slurry

The present latent-heat microcapsules were produced by encapsulating *n*-octacosane of paraffin wax as a latent-heat storage material with melamine resin by an in-situ polymerization method. Figure 1 shows the variation of the heat evolved from *n*-octacosane with temperature cooled at a velocity of 2.0 K/min, determined using a differential scanning calorimeter. The results in Fig. 1 reveal that the melting and transition points of *n*-octacosane are T_{mp} =334.7 K (latent heat L_{mp}=164.6 kJ/kg) and T_{tp}= 319.3 K (transition heat L_{tp}=39.8 kJ/kg), respectively and the total heat ($L_{mp}+L_{tp}$) evolved was estimated to be 204.4 kJ/kg. The particle diameter of latent-heat microcapsules was measured using an optical micrograph with a magnification of 1 000. The diame-

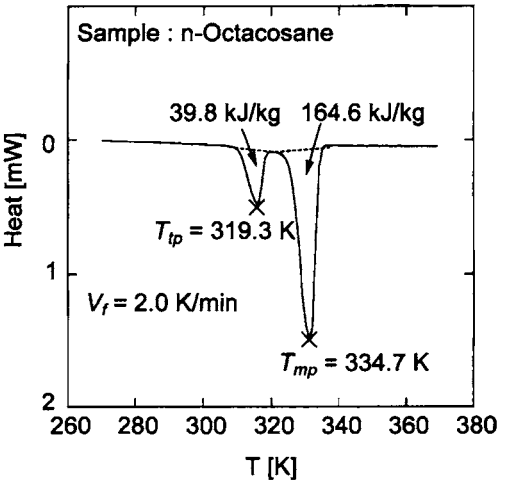

Fig. 1 DSC curve

ter of the microcapsules varied from 0.1 μm to 3.0 μm and the arithmetic diameter was d_{pm}=1.2 μm. The latent-heat microcapsule slurry was white in color with good fluidity, and the homogeneous dispersion of latent-heat microcapsules in water persisted for over 3 000 hours[5]. The concentration of latent-heat microcapsules varied from C_{mi}=11.0 mass% (concentration of water C_w=89 mass%, concentration of *n*-octacosane C_t=9.9 mass%, concentration of surfactant C_s=1.1 mass%) to 44 mass% (C_w=56.0 mass%, C_t=39.6 mass%, C_s=4.4 mass%). The physical properties of latent-heat microcapsule slurry C_{mi}=44 mass% under the solid (*s*) and liquid (*l*) conditions of *n*-octacosane are presented as follows: density; ρ_s=1 180 kg/m³, ρ_l=982 kg/m³, thermal conductivity; λ_s=0.442 W/(m·K), λ_l=0.412 W/(m·K), specific heat; Cp_s=3.12 kJ/(kg·K), Cp_l=3.21 kJ/(kg·K), apparent viscosity; η=91 mPs·s at 349 K.

3. Experimental Apparatus and Procedure

Figure 2 shows the schematic of the experimental apparatus and the detail of nozzles. The experimental apparatus consisted mainly of a test section of a heat storage vessel packed with latent-heat microcapsule slurry and an air quality control system for supplying hot air to the latent-heat microcapsule slurry. In the air quality control system, the flow rate pulsation of the air pressurized by a compressor was calmed using the buffer tank. The air-flow rate was controlled by the flow-regulating valve, and it was measured with a mass flowmeter (measuring accuracy of ±3.0%). The air temperature and humidity before charging the hot air to the test section via circular nozzles were controlled at desired values by operating an electric heater and a bubble tower humidifier. The air bubbles generated from the circular nozzles ascended into a latent-heat microcapsule slurry layer in the test section for heat storage. The test section was constructed of a rectangular vessel (a cross section of 100 mm×100 mm, a maximum height of 500 mm). The rectangular heat storage vessel consisted of the transparent acrylic plate (10 mm in thickness) for observing the flow behavior of air bubbles and the microcapsule slurry. The rectangular vessel was covered with an insulating material of 50 mm thickness for lessening the heat loss to the environment except during visual observation. The inlet and outlet air temperatures, T_{ain} and T_{aout}, and humidities, ϕ_{ain} and ϕ_{aout}, of the test section were measured with K-type thermocouples of 0.32 mm diameter (measuring accuracy of ±0.2 K) and polymer-film-type hygrometers (measuring accuracy of ±0.5%), respectively. The inlet air pressure was also measured with a precision pressure gage (measuring accuracy of ±0.02 kPa). The thermocouple for T_{aout} was set into a reduced section made of thermal insulation material. A stainless steel wire mesh (12 mesh, diameter of 0.1 mm) was installed between the surface of the latent-heat microcapsule slurry layer and the reduction section for preventing water droplets from adhering to the thermocouple and hygrometer sensor. The circular nozzles of 1 mm diameter, as shown in the lower part of Fig. 2, were mounted on the bottom of the test section at intervals of 10 mm with in-line arrangement for avoiding the interaction of air bubbles near the nozzles and for homogeneous flow behavior of ascending air bubbles in the latent-heat microcapsule slurry. The hydrodynamic diameter of ascending air bubbles at a position 20 mm from the nozzle level was estimated to range from 1.8 to 4.5 mm. A hydraulic filter (thickness of 0.55 mm, void ratio of 54%) was mounted under the nozzle plate in order to prevent the microcapsule slurry from leaking. The latent-heat microcapsule slurry as a test sample was maintained at 303.2 K below the transition temperature of 319.3 K in order to solidify completely *n*-octacosane encapsulated with the melamine resin shell as a latent-heat storage material in a constant temperature controlled bath. After that, the latent-heat microcapsule slurry was packed into the test section, as shown in Fig. 2. The representative temperature of the microcapsule slurry was measured with a T-type thermocouple

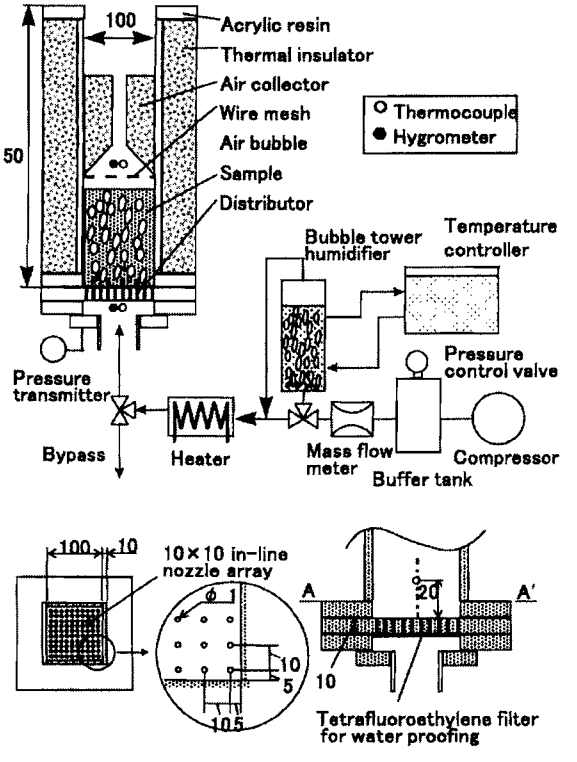

Fig. 2 Schematic diagram of experimental apparatus

(wire diameter of 0.32 mm, measuring accuracy of ±0.2 K) at the vertical position of 20 mm from the nozzle level. The experimental data were obtained under the following conditions.

- concentration of latent-heat storage material: C_{mi}=11.0 - 44.0 mass%
- initial height of latent-heat microcapsule slurry layer: Z_i=0.05 - 0.15 m
- superficial airflow velocity: V_o=1.7×10^{-2} - 6.7×10^{-2} m/s
- inlet air temperature: T_{ain}=353.2 - 373.2 K
- inlet air relative humidity: ϕ_{ain}=5 - 80 RH%
- inlet air absolute humidity: X_{ain}=0.0065 - 0.30 kg/kg'

4. Experimental Results and Discussion

4.1 Latent-heat microcapsule slurry layer height behavior in the presence of air bubbles

The total volume of air bubbles remaining in the latent-heat microcapsule slurry layer is an important factor for evaluating the amount of latent-heat storage from air bubbles ascending to the latent-heat microcapsules. The holdup ε which denotes the volume fraction of air bubbles in the microcapsule slurry layer was estimated by analyzing the visualization photographs. Figure 3 shows the relationship between hold-up ε and superficial airflow velocity V_o at a height of Z_i=0.10 m for various concentrations of n-octacosane C_{mi} and water only (closed circles). In Fig. 3, it is seen that the values of ε for latent-heat microcapsule slurry increase with an increase in superficial airflow velocity V_o and these values are, to a great extent, above the values of water. These results ε of are explained by the fact that the value of ε is influenced by a momentum balance among buoyancy of air bubbles, surface tension and viscosity of the microcapsule slurry. That is, high viscosity of the microcapsule slurry results in increasing the hold-up, as compared with results of water.

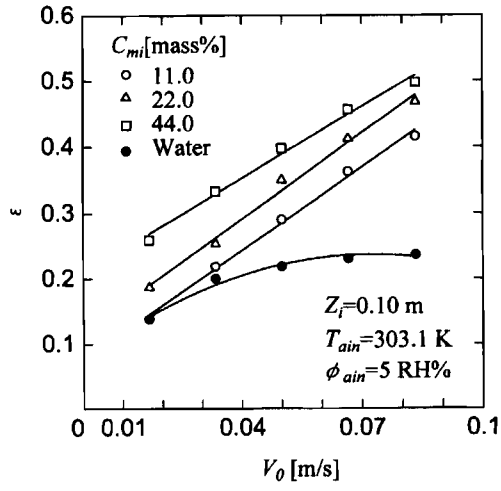

Fig. 3 Variation of ε with V_o

Figure 4 presents time histories of outlet air temperature T_{aout} and relative humidity ϕ_{aout}, and the microcapsule slurry temperature T_c at an inlet air temperature of T_{ain}=356.2 K and relative humidity of ϕ_{ain}=60 RH%. In this study, the initial temperature of the microcapsule slurry was set at 303.2 K below the transition temperature T_{tp}=319.3 K of the latent-heat storage material (n-octacosane). From Fig. 4, it is noted that the value of T_c increases markedly due to the sensible heat storage for 7.5 min from the start of the test run. For this time period, it is seen that the rate of increase of T_c with time is reduced at approximately T_c=319.3 K due to the transition heat evolved, and after t=10 min the value of T_c increases gradually with time during evolution of the latent heat at approximately T_{mp}=334.7 K. On the other hand, it is assumed that the higher heat exchange efficiency is obtained by the direct-contact heat exchange between air bubbles and the microcapsule slurry, since the outlet air temperature T_{aout} becomes almost the same as the microcapsule slurry temperature T_c with time. It is also seen that the value of ϕ_{aout} increases markedly and then approaches the saturated moist air condition due to the high mass transfer coefficient by the direct-contact mass transfer between air bubbles and the microcapsule slurry.

4.2 Variation of heat transferred between air bubbles and the heat storage material with time

Figure 5 presents the variation of the heat obtained by the latent-heat storage material and the transmitted heat for each element with time under the same experimental conditions as those indicated in Fig. 4. The amount of latent-heat storage integrated with time Q_{mit} was calculated by the energy balance

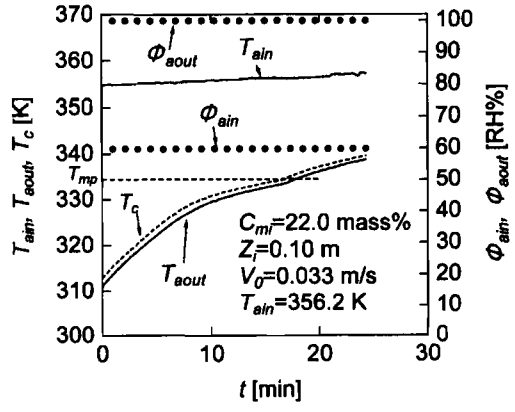

Fig. 4 Time history of measured values

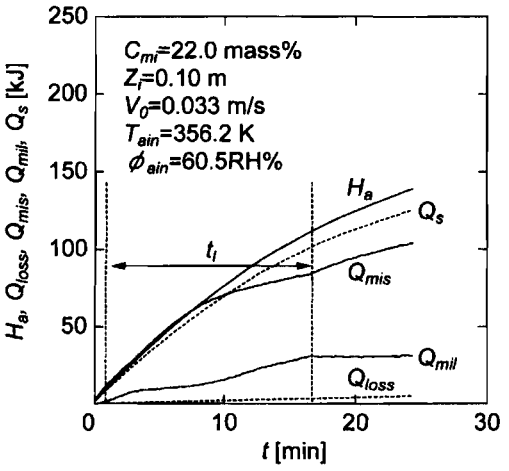

Fig. 5 Time history of exchanged heat

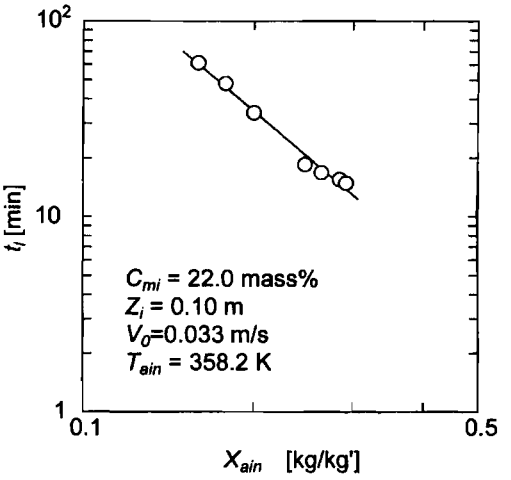

Fig. 6 Variation of t_l with X_{ain}

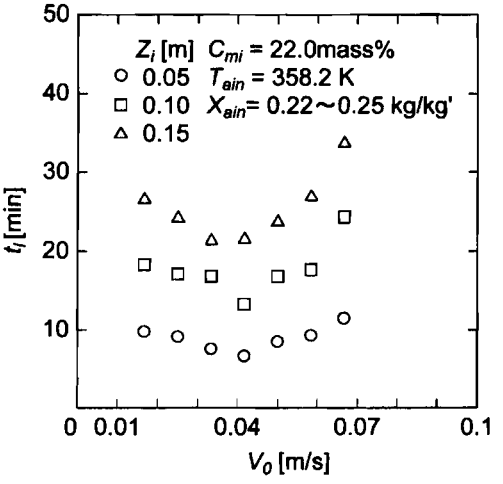

Fig. 7 Variation of t_l with V_o

among the enthalpy differences integrated with time between inlet air and outlet air H_a, heat loss integrated with time Q_{loss} and sensible heat of the microcapsule slurry integrated with time Q_{mis} as follows:

$$Q_{mil}=H_a-Q_{loss}-Q_v-Q_{mis} \quad (1)$$

where Q_v refers to the sensible heat of the heat storage vessel integrated with time. The completion time of latent-heat storage in the microcapsule slurry was estimated as the time period when the value of Q_{mil} is equal to the total latent heat $m_{mi}L$ by using the following equation.

$$m_{mi}L=Q_{mil}=\int_0^{t_l}(\Delta\dot{H}_a-\dot{Q}_{loss}-\dot{Q}_v-\dot{Q}_{mis})dt \quad (2)$$

here, the superscript $\cdot$ denotes the heat per time.

The value of Q_{loss} in Eq.(2) was estimated from the results obtained in the preliminary heat storage experiments which were carried out to measure the heat loss from the heat storage vessel to the environment using water instead of the microcapsule slurry. The value of enthalpy difference between inlet air and outlet air ΔH_a is defined as follows:

$$\Delta\dot{H}_a=\dot{H}_{ain}-\dot{H}_{aout}$$
$$=[Cp_aT_{ain}+(r+Cp_sT_{ain})X_{ain}]$$
$$-[Cp_aT_{aout}+(r+Cp_sT_{ain})X_{aout}]\cdot\dot{m}_a \quad (3)$$

In Fig. 5, it is found that the value of sensible heat stored Q_{mis} increases to a great extent in the temperature range below the melting point of latent-heat storage material with time by 7.5 min after starting the test run, and this rate of increase of Q_{mis} with time is reduced at temperatures over the melting point of 334.7 K. It is seen that the value of latent-heat stored Q_{mil} increases gradually from t=1.5 min to 17 min during evolution of the latent heat by a phase change. The value of t_l in Fig. 5 denotes the completion time period of the latent heat storage process. The ascending air bubbles are discharged outside under the almost saturated moist air condition from the microcapsule slurry layer with supply of heat to the microcapsule slurry by direct-contact heat transfer. The value of Q_s in Fig. 5 indicates the time-integrated latent heat evolved by the condensation of water vapor in ascending air bubbles. Under the present experimental conditions, this is revealed by the fact that the value of Q_s accounts for more than ninety percent of the enthalpy difference of inlet and outlet moist air. Therefore, it is important to consider the absolute humidity difference between inlet and outlet air.

4.3 Completion time period of latent-heat storage process

Figure 6 presents the variation of absolute humidity of inlet air X_{ain} with the completion time period of latent-heat storage t_l. It is found that an increase in absolute humidity of inlet air enables the shortening of the completion time period t_l by the addition of the

latent heat based on water vapor condensation. Figure 7 shows the relationship between the completion time period of latent-heat storage t_l and superficial airflow velocity for various initial heights of the microcapsule slurry layer Z_i. The results in Fig. 7 show that the value of t_l decreases with increasing superficial airflow velocity V_o, reaches a local minimum of t_l at approximately $V_o=0.040$ m/s, and finally increases with an increase in V_o over $V_o=0.040$ m/s. In the low-velocity range of $V_o<0.040$ m/s, the decrease in t_l can be explained by the fact that most of the heat occupied by air bubbles, that is, the heat capacity of air bubbles which is proportional to superficial airflow velocity V_o, is transmitted into the microcapsule slurry. On the other hand, in the high-velocity range of $V_o>0.040$ m/s, the increase in t_l can be brought about by means of decreasing the heating surface area and shortening the staying time of air bubbles in the microcapsule slurry layer due to the combination of air bubbles generated from circular nozzles. Therefore, the correlation of temperature efficiency, enthalpy difference between inlet and outlet air and the completion time period of latent-heat storage can be classified into two ranges.

4.4 Temperature efficiency of latent-heat storage vessel

One of the important parameters in estimating the effect of direct-contact heat transfer is the temperature characteristic of outlet air from the microcapsule slurry layer. It was understood that the outlet air temperature T_{aout} varied with time, as shown in Fig. 4. In the present study, an arithmetic time average of outlet air temperature T_{aout} was used as a representative temperature of outlet air. Temperature efficiency θ including the value of T_{aout} is defined as follows:

$$\theta=\frac{T_{ain}-\overline{T}_{aout}}{T_{ain}-T_{tp}} \tag{4}$$

where the value of T_{tp} refers to the transition point temperature of latent-heat storage material.

The viscosity of the microcapsule slurry appears to be an important factor in the flow behavior of air bubbles in the microcapsule slurry layer. This viscosity is dependent on the concentration of the latent-heat storage material C_{mi}. Therefore, the first nondimensional parameter which exerts an influence on the temperature efficiency θ should be the percentage concentration of the latent-heat storage material $C^*(C_{mi}/100)$. The ratio of height Z_l of the microcapsule slurry layer to the average diameter d_{pm} of microcapsules $Z^*(=Z_l/d_{pm})$ was used as the second nondimensional parameter for temperature efficiency, which was related to the staying time period of air bubbles in the microcapsule slurry layer.

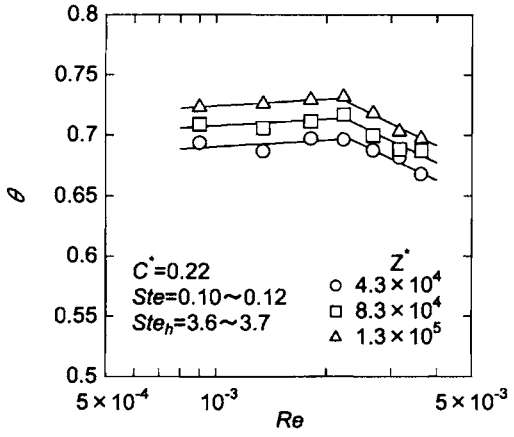

Fig. 8 Variation of Re with θ

$$Z^*=\frac{Z_i}{d_{pm}} \tag{5}$$

The Reynolds number Re based on a superficial airflow velocity was utilized as the third nondimensional parameter and indicates the effect of the injected airflow rate on the temperature efficiency. The average diameter of the microcapsules was used as a representative dimension such as for the fluidized bed model[6].

$$Re=\frac{V_0\cdot d_{pm}}{v_a} \tag{6}$$

The Stefan number Ste was adopted as the fourth nondimensional parameter and represented the temperature difference between inlet air and melting point temperature of latent-heat storage material.

$$Ste=\frac{Cp_a(T_{ain}-T_{mp})}{L} \tag{7}$$

Here, L denotes the total of transient (crystal structure change) heat and latent (liquid-solid phase change) heat.

On the other hand, the modified Stefan number Ste_h was defined for humidity of the inlet air by using the enthalpy of inlet air as follows:

$$Ste_h=\frac{\{r+Cp_a(T_{ain}-T_{mp})\}\cdot X_{ain}}{L} \tag{8}$$

Figure 8 shows the variation of temperature efficiency θ for Reynolds number Re for various ratios of Z^*. The value of θ increases gradually with an increase in Re in the range of $Re=0.9\times10^{-3}$ - 2.3×10^{-3}. This increase in θ is explained by the fact that the increase in the heat transmitted from air bubbles to the microcapsule slurry with an increase in airflow rate leads to a decrease in the outlet air temperature T_{aout}, since the staying time period of air bubbles increases with increase of the hold-up of the microcapsule slurry layer. In contrast, it is found that the value of θ decreases with an increase in Re in the range of $Re=2.3\times10^{-3}$ - 4.8×10^{-3}. This decrease in θ

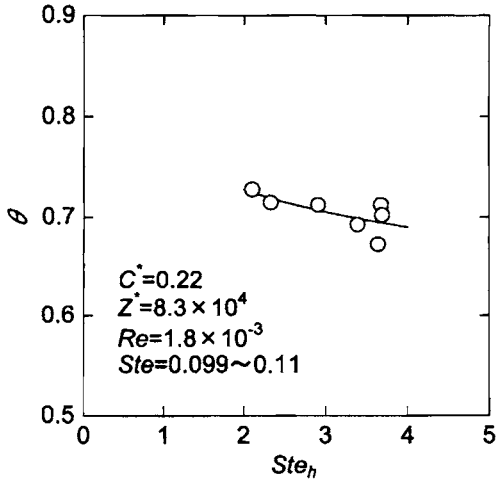

Fig. 9 Variation of Ste_h with θ

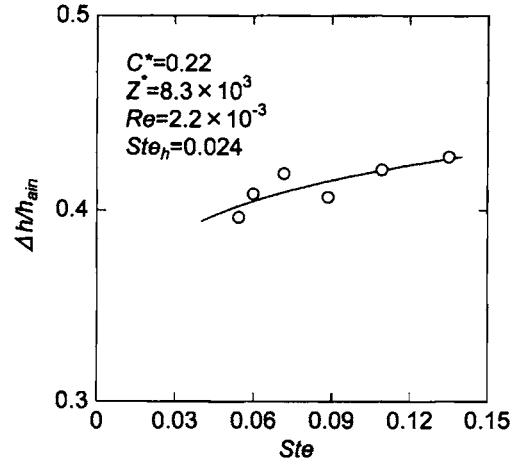

Fig. 10 Variation of Ste with $\Delta h/h_{ain}$

is explained by the fact that the heat transmitted from air bubbles to the microcapsule slurry decreases with increasing airflow rate since the combination of air bubbles results in the enlargement of air bubble size with increasing airflow velocity, that is, airflow rate. The results for the parameter of Z^* reveal that the value of θ increases with an increase in Z^* since an increase in the contact time period between air bubbles and the microcapsule slurry with increasing Z^* leads to an increase in the amount of heat transferred between them.

Figure 9 shows the relationship between the temperature efficiency of θ and the modified Stefan number Ste_h. The results in Fig. 9 indicate that the value of θ decreases with increasing Ste_h. Based on the effects of these parameters on θ, the following correlation equations (9) and (10) were derived by the root mean squared method within a standard deviation of $\pm 11.2\%$.

For $Re=0.9\times10^{-3}$ - 2.3×10^{-3}:

$$\theta=0.97\times C^{*-0.052}Z^{*0.039}Re^{0.011}Ste^{0.29}Ste_h^{-0.080} \quad (9)$$

For $Re=2.3\times10^{-3}$ - 3.6×10^{-3}:

$$\theta=0.51\times C^{*-0.052}Z^{*0.039}Re^{-0.092}Ste^{0.29}Ste_h^{-0.080} \quad (10)$$

These equations are applicable in the following parameter ranges:

$C^*=0.11$ - 0.44, $Z^*=4.1\times10^4$ - 1.3×10^5,

$Ste=0.054$ - 0.14, $Ste_h=2.1$ - 3.7.

4.5 Variation in enthalpy difference between inlet and outlet air

The variation in enthalpy difference of air bubbles through the microcapsule slurry layer was examined in the present study. Figure 10 shows the relationship between the ratio of enthalpy difference Δh between inlet and outlet air to the enthalpy of inlet air h_{ain} and Stefan number Ste. The value of Δh was calculated by the following:

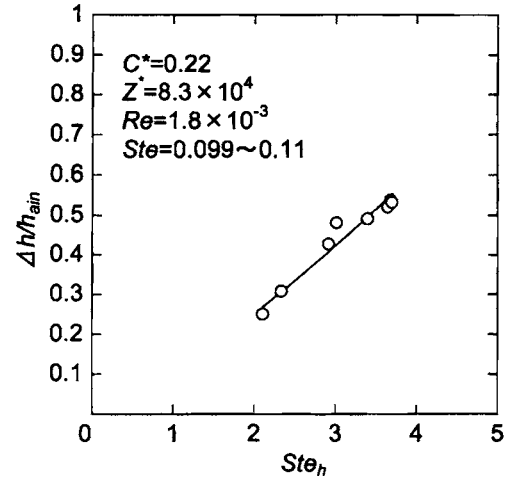

Fig. 11 Variation of Ste_h with $\Delta h/h_{ain}$

$$\Delta h=\{Cp_aT_{ain}+(r+Cp_sT_{ain})X_{ain}\}-\{Cp_aT_{aout}+(r+Cp_sT_{aout})X_{aout}\} \quad (11)$$

The results in Fig. 10 indicate that the value of $\Delta h/h_{ain}$ increases with increasing Stefan number Ste. This increase in $\Delta h/h_{ain}$ could be explained by the fact that the inlet air temperature exerts less of extent an influence on the enthalpy of outlet air, due to the fact that a smaller amount of sensible heat contributes to the enthalpy. Moreover, the increase in enthalpy of inlet air, that is, the increase in Stefan number, leads to an increase in enthalpy difference Δh. As a result, the value of $\Delta h/h_{ain}$ increases with increasing Stefan number Ste. Figure 11 presents the variation of $\Delta h/h_{ain}$ with the modified Stefan number Ste_h. In Fig. 11, it is noted that the value of $\Delta h/h_{ain}$ increases with an increase in Ste_h. This tendency of $\Delta h/h_{ain}$ is due to the fact that variation in the humidity of air greatly affects the heat and mass transfer by the latent heat evolved with a phase change, in comparison with the

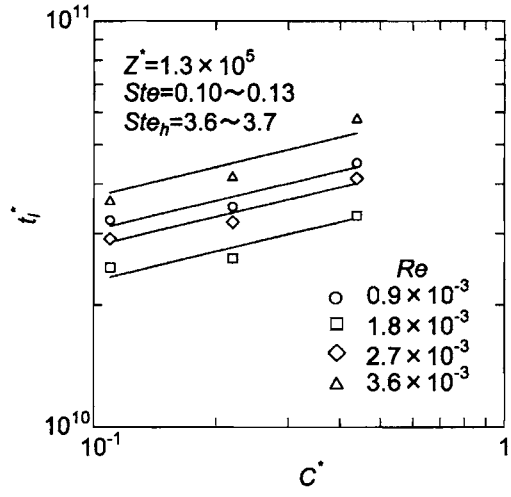

Fig. 12 Variation of C^* with t_i^*

variation in temperature, that is, sensible heat. The correlation equations of $\Delta h/h_{ain}$ were derived by the root mean squared method within a standard deviation of ±15.4% as follows.

For the range of $Re=9.9\times10^{-3}$ - 2.3×10^{-3}:

$$\Delta h/h_{ain}=0.088\times C^{*-0.037}Z^{*0.049}Re^{0.014}Ste^{0.10}Ste_h^{1.2} \quad (12)$$

For the range of $Re=2.3\times10^{-3}$ - 3.6×10^{-3}:

$$\Delta h/h_{ain}=0.040\times C^{*-0.037}Z^{*0.049}Re^{-0.12}Ste^{0.10}Ste_h^{1.2} \quad (13)$$

These equations are applicable in the following parameter range:

$C^*=0.11$ - 0.44, $Z^*=4.1\times10^4$ - 1.3×10^5,

$Ste=0.054$ - 0.14, $Ste_h=2.1$ - 3.7.

4.6 Nondimensional correlation of completion time period for latent heat storage

Investigations were carried out on the completion time period t_i of latent-heat storage in the present study, which is an important factor for estimating the efficiency of latent-heat storage. Nondimensional completion time period t_i^* of latent-heat storage is defined as follows:

$$t_i^*=\frac{t_i\cdot a_c}{d_{pm}^2} \quad (14)$$

Figure 12 shows the variation of nondimensional completion time period t_i^* with concentration of latent-heat material C^* for various Reynolds numbers Re. In Fig. 12, it is found that the value of t_i^* increases with an increase in C^* due to an increase in the amount of latent heat with increasing C^*. Figure 13 presents the relationship between nondimensional time period t_i^* and Stefan number Ste. The results of Fig. 13 show that the value of t_i^* decreases with increasing Ste, that is, inlet air temperature T_{ain}. This decrease in t_i^* could be caused by the increase in the amount of heat transmitted due to the increase in

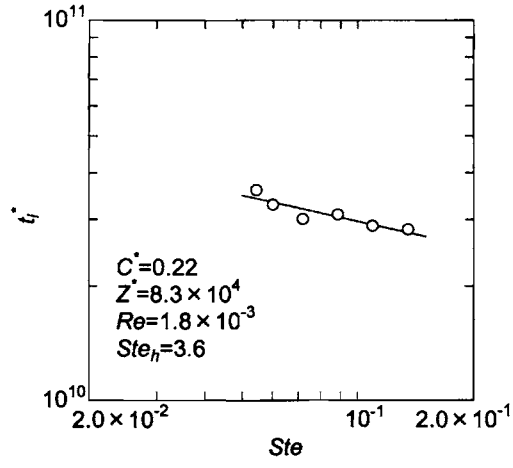

Fig. 13 Variation of Ste with t_i

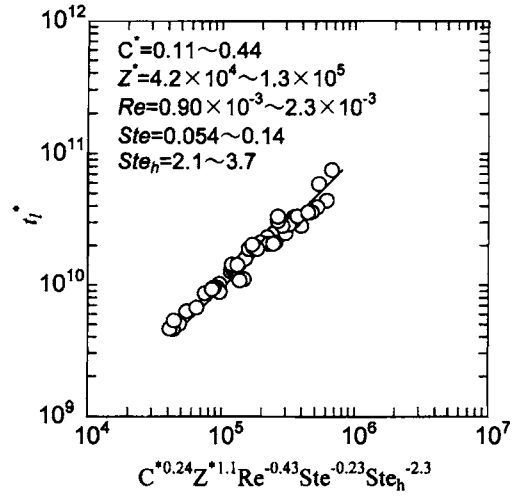

Fig. 14 The nondimensional correlation equations for t_i^* ($Re=0.9\times10^{-3}$ - 2.3×10^{-3})

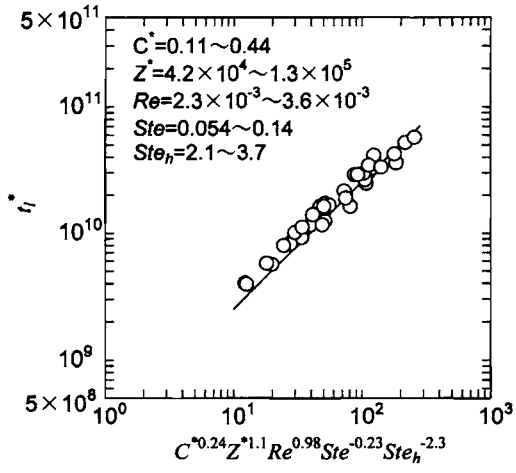

Fig. 15 The nondimensional correlation equations for t_i^* ($Re=2.3\times10^{-3}$ - 3.6×10^{-3})

the temperature difference between air bubbles and the microcapsule slurry with rising inlet air temperature. From the results in Figs. 12 and 13, the nondimensional correlation equations of completion time period of latent-heat storage were derived by the root mean squared method within a standard deviation of ±11% as follows.

For the range of $Re=0.9\times10^{-3}$ - 2.3×10^{-3}:

$$t_i^*=9.2\times10^4 C^{*0.24} Z^{*1.1} Re^{-0.43} Ste^{-0.23} Ste_h^{-2.3} \quad (15)$$

For the range of $Re=2.3\times10^{-3}$ - 3.6×10^{-3}:

$$t_i^*=2.7\times10^8 \cdot C^{*0.24} \cdot Z^{*1.1} \cdot Re^{0.98} Ste^{-0.23} Ste_h^{-2.3} \quad (16)$$

These equations are applicable in the following parameter range:

$C^*=0.11$ - 0.44, $Z^*=4.1\times10^4$ - 1.3×10^5,

$Ste=0.054$ - 0.14, $Ste_h=2.1$ - 3.7.

Figures 14 and 15 show the variation of t_i^* with nondimensional parameters defined in Eqs.(14) and (15).

5. Concluding Remarks

We proposed a new type of latent-heat storage system containing a microcapsule slurry, which was composed of a mixture of fine encapsulated particles of paraffin wax and water, by a direct-contact heat exchange method in which the heat was stored from hot air bubbles to the microcapsule slurry for a domestic heating and cooling system. The effects of some parameters on latent heat storage characteristics were clarified experimentally as follows.

(1) The results revealed that the greater part of the heat transmitted from hot air bubbles to the microcapsule slurry was latent heat based on the variation in humidity of air bubbles in comparison with sensible heat based on variations in air temperature.

(2) It was found that a higher efficiency of mass and heat transfer was obtained by direct-contact heat exchange between air bubbles and the microcapsule slurry.

(3) The nondimensional correlation equations of the completion time period of latent heat storage, temperature efficiency and enthalpy difference between inlet and outlet air were derived by some nondimensional parameters.

Acknowledgements

The authors would like to thank Mr. Mamoru Ishiguro of Mitsubishi Paper Mills Limited, for his providing the latent-heat microcapsule sample.

References

(1) Inaba, H., Journal of JSME, (in Japanese), Vol. 98, No. 925 (1995), pp. 999-1000.

(2) Inaba. H., Journal of Refrigeration, (in Japanese), Vol. 71, No. 830 (1996), pp. 1346-1358.

(3) Inaba, H., Trans. of JSME, (in Japanese), Vol. 59, No. 565, B (1993), pp. 2882-2889.

(4) Kondo, Y., Microcapsule, (in Japanese), (1991), pp. 24-26, Japan Standard Association, Tokyo.

(5) Inaba, H. and Morita, S., Trans. Jpn. Soc. Mech. Eng., (in Japanese), Vol. 61, No. 592, B (1995), pp. 4448-4454.

(6) Chiba, S. and Yoshida, K., An Outline of Fluidized Bed, (in Japanese), (1996), pp. 41-46, Asakura Book Pub. Co. Tokyo.